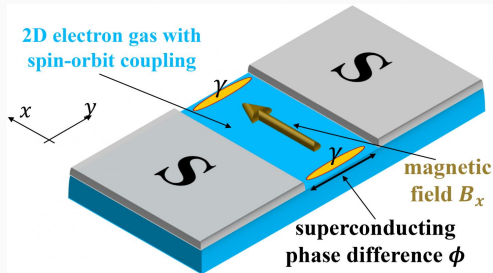


Josephson junctions: a platform for exotic superconducting phases

Tadeusz Domański

M. Curie-Skłodowska Univ.



OUTLINE

1. Josephson effect

2. Josephson junctions

(some applications & recent advancements)

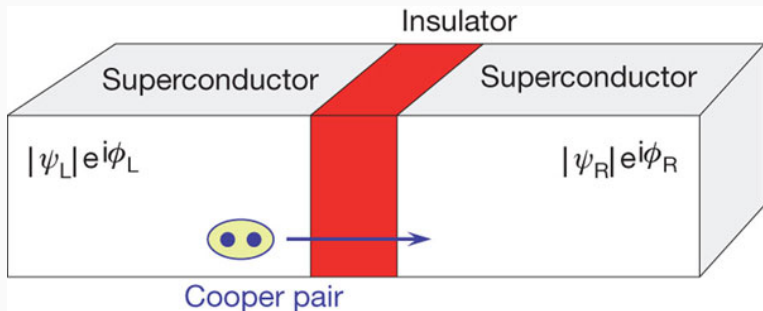
3. Topological superconductivity

(interplay of magnetism and electron pairing)

Part 1. Josephson effect (prediction & discovery)

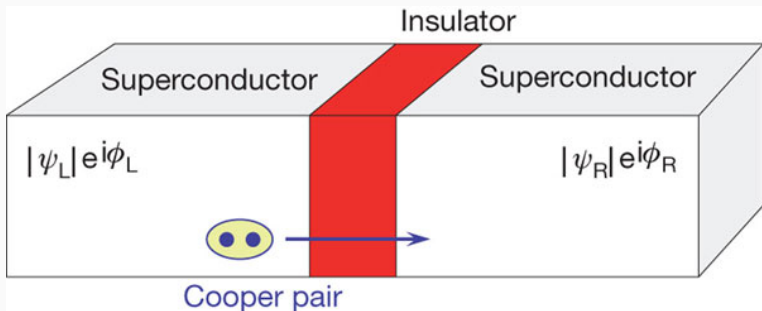
JOSEPHSON EFFECT

Two superconductors, differing in phase $\phi_L \neq \phi_R$, contacted through a narrow ($\leq \xi$) insulating region induce *superflow* of the Cooper pairs.



JOSEPHSON EFFECT

Two superconductors, differing in phase $\phi_L \neq \phi_R$, contacted through a narrow ($\leq \xi$) insulating region induce *superflow* of the Cooper pairs.



Effect has been predicted by B.D. Josephson in 1962.

/ 22-year-old PhD student at Cambridge, England /

HYDRODYNAMIC REASONING

In quantum mechanics the probability current is defined by

$$\vec{j}(\vec{r}, t) = -\frac{i\hbar}{2m} [\Psi^*(\vec{r}, t) \nabla \Psi(\vec{r}, t) - \Psi(\vec{r}, t) \nabla \Psi^*(\vec{r}, t)]$$

HYDRODYNAMIC REASONING

In quantum mechanics the probability current is defined by

$$\vec{j}(\vec{r}, t) = -\frac{i\hbar}{2m} [\Psi^*(\vec{r}, t) \nabla \Psi(\vec{r}, t) - \Psi(\vec{r}, t) \nabla \Psi^*(\vec{r}, t)]$$

Applying this formalism to the wave-function Φ_0 of Cooper pairs

$$\Phi_0(\vec{r}, t) \equiv \underbrace{|\Phi_0(\vec{r}, t)|}_{\sqrt{n(\vec{r}, t)}} e^{i\phi(\vec{r}, t)}$$

HYDRODYNAMIC REASONING

In quantum mechanics the probability current is defined by

$$\vec{j}(\vec{r}, t) = -\frac{i\hbar}{2m} [\Psi^*(\vec{r}, t) \nabla \Psi(\vec{r}, t) - \Psi(\vec{r}, t) \nabla \Psi^*(\vec{r}, t)]$$

Applying this formalism to the wave-function Φ_0 of Cooper pairs

$$\Phi_0(\vec{r}, t) \equiv \underbrace{|\Phi_0(\vec{r}, t)|}_{\sqrt{n(\vec{r}, t)}} e^{i\phi(\vec{r}, t)}$$

we can express the Josephson current density

$$\vec{j}_J(\vec{r}, t) = -q \frac{i\hbar}{2m} [\Phi_0^* \nabla \Phi_0 - \Phi_0 \nabla \Phi_0^*]$$

HYDRODYNAMIC REASONING

In quantum mechanics the probability current is defined by

$$\vec{j}(\vec{r}, t) = - \frac{i\hbar}{2m} [\Psi^*(\vec{r}, t) \nabla \Psi(\vec{r}, t) - \Psi(\vec{r}, t) \nabla \Psi^*(\vec{r}, t)]$$

Applying this formalism to the wave-function Φ_0 of Cooper pairs

$$\Phi_0(\vec{r}, t) \equiv \underbrace{|\Phi_0(\vec{r}, t)|}_{\sqrt{n(\vec{r}, t)}} e^{i\phi(\vec{r}, t)}$$

we can express the Josephson current density

$$\vec{j}_J(\vec{r}, t) = - q \frac{i\hbar}{2m} [\Phi_0^* \nabla \Phi_0 - \Phi_0 \nabla \Phi_0^*] = q n(\vec{r}, t) \underbrace{\frac{\hbar}{m} \nabla \phi(\vec{r}, t)}_{\vec{v}(\vec{r}, t)}$$

HYDRODYNAMIC REASONING

In quantum mechanics the probability current is defined by

$$\vec{j}(\vec{r}, t) = - \frac{i\hbar}{2m} [\Psi^*(\vec{r}, t) \nabla \Psi(\vec{r}, t) - \Psi(\vec{r}, t) \nabla \Psi^*(\vec{r}, t)]$$

Applying this formalism to the wave-function Φ_0 of Cooper pairs

$$\Phi_0(\vec{r}, t) \equiv \underbrace{|\Phi_0(\vec{r}, t)|}_{\sqrt{n(\vec{r}, t)}} e^{i\phi(\vec{r}, t)}$$

we can express the Josephson current density

$$\vec{j}_J(\vec{r}, t) = - q \frac{i\hbar}{2m} [\Phi_0^* \nabla \Phi_0 - \Phi_0 \nabla \Phi_0^*] = q n(\vec{r}, t) \underbrace{\frac{\hbar}{m} \nabla \phi(\vec{r}, t)}_{\vec{v}(\vec{r}, t)}$$

where $q = 2e$ is charge and $\vec{v}(\vec{r}, t)$ is velocity of Cooper pairs.

PROBABLE OBSERVATION OF THE JOSEPHSON SUPERCONDUCTING TUNNELING EFFECT

P. W. Anderson and J. M. Rowell
Bell Telephone Laboratories, Murray Hill, New Jersey
(Received 11 January 1963)

EXPERIMENTAL EVIDENCE

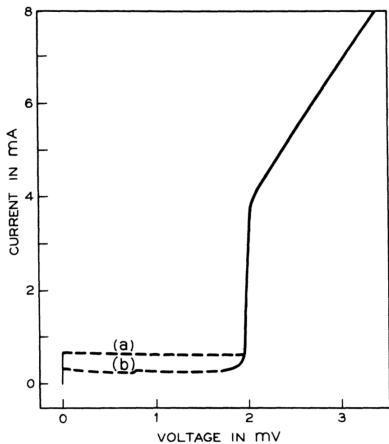
VOLUME 10, NUMBER 6

PHYSICAL REVIEW LETTERS

15 MARCH 1963

PROBABLE OBSERVATION OF THE JOSEPHSON SUPERCONDUCTING TUNNELING EFFECT

P. W. Anderson and J. M. Rowell
Bell Telephone Laboratories, Murray Hill, New Jersey
(Received 11 January 1963)



Authors reported on:

„dc tunneling current at or near zero voltage in very thin tin oxide barriers between superconducting Sn and Pb”

NOBEL PRIZE IN PHYSICS

1973

B.D. Josephson (with L. Esaki & I. Giaver)

NOBEL PRIZE IN PHYSICS

1973

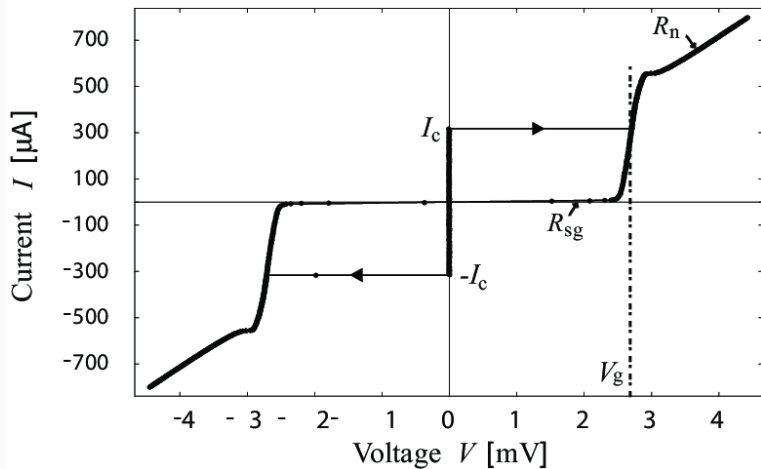
B.D. Josephson (with L. Esaki & I. Giaver)

1972

J. Bardeen, L.N. Cooper, J.R. Schrieffer

I(V) CHARACTERISTICS

Typical current-voltage plot, where $V_g = 2\Delta$

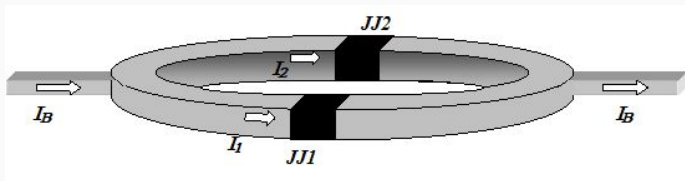


Part 2. Josephson junctions

(applications & recent advancements)

1. QUANTUM INTERFEROMETER DEVICE

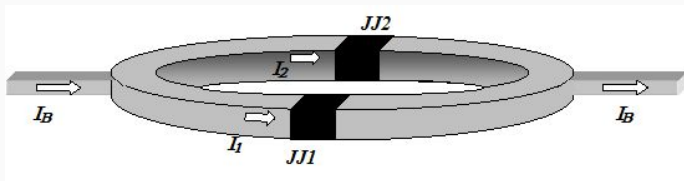
SQUID - superconducting quantum interferemoreter device



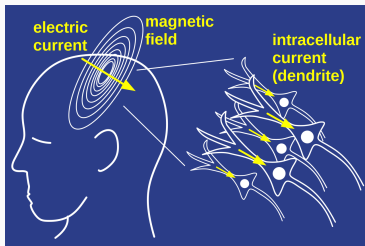
This device allows for an extremely precise detection of magnetic fields

1. QUANTUM INTERFEROMETER DEVICE

SQUID - superconducting quantum interferemoreter device



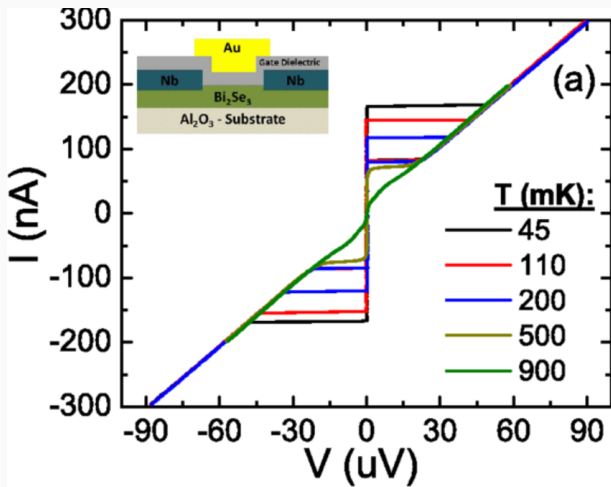
This device allows for an extremely precise detection of magnetic fields



capable to probe the neural currents in a human brain !

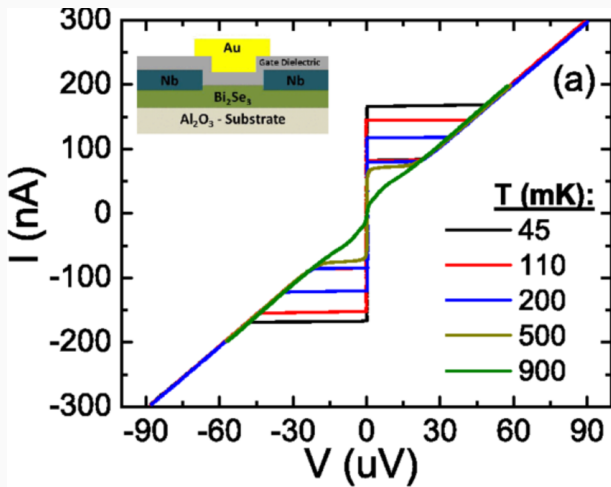
2. RESISTIVE TRANSITION

Critical dc current I_c diminishes upon increasing temperature,



2. RESISTIVE TRANSITION

Critical dc current I_c diminishes upon increasing temperature,



when Josephson current switches from superflow to resistive behaviour.

2. ULTRAFAST THERMOMETRY

A weak link (Aluminum Dayem nanobridge) probed with nanosecond current (pump-and-probe) pulses can serve as a temperature-sensing element

2. ULTRAFAST THERMOMETRY

A weak link (Aluminum Dayem nanobridge) probed with nanosecond current (pump-and-probe) pulses can serve as a temperature-sensing element

PHYSICAL REVIEW APPLIED **10**, 044068 (2018)

Nanosecond Thermometry with Josephson Junctions

M. Zgirski,^{1,*} M. Foltyn,¹ A. Savin,² K. Norowski,¹ M. Meschke,² and J. Pekola²

¹*Institute of Physics, Polish Academy of Sciences, Aleja Lotnikow 32/46, 02-668 Warsaw, Poland*

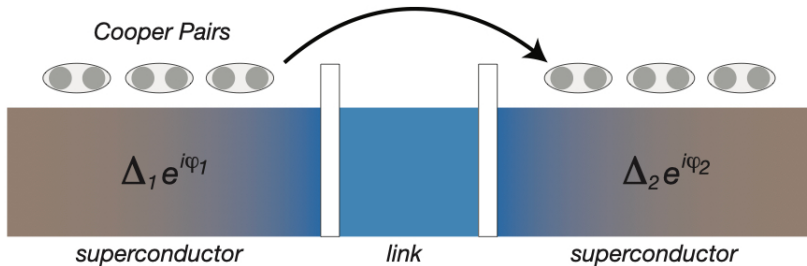
²*Low Temperature Laboratory, Department of Applied Physics, Aalto University School of Science, P.O. Box 13500, FI-00076 Aalto, Finland*

Measurements delivered resolution better than 10 ns !

3. PHASE-PERIODICITY OF JOSEPHSON CURRENT

Superflow of the Cooper pairs is driven by phase difference, therefore dc current has (usually) 2π -periodicity with respect to $\phi = \phi_L - \phi_R$.

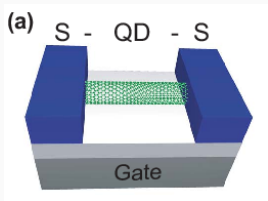
Josephson Junctions



$$I_S = I_C \sin(\varphi)$$

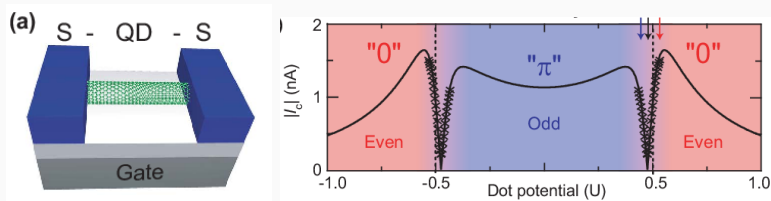
3. CURRENT REVERSAL IN NANOJUNCTIONS

Carbon nanotube interconnecting two superconductors, differing in phase.



3. CURRENT REVERSAL IN NANOJUNCTIONS

Carbon nanotube interconnecting two superconductors, differing in phase.

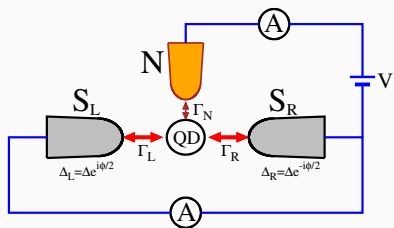


At certain gate potential the dc Josephson current abruptly changed its magnitude and direction (zero-pi transition).

H.I. Jorgensen, T. Novotný, K. Grove-Rasmussen, K. Flensberg, P.E. Lindelof, NanoLett. 7, 2441 (2007).

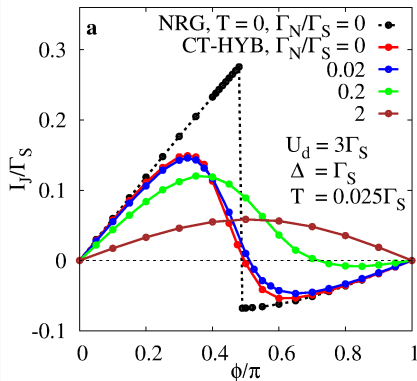
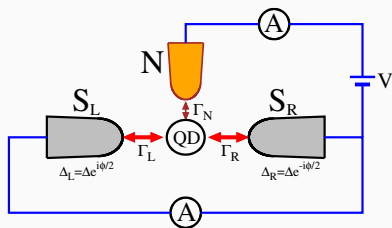
3. JOSEPHSON CURRENT REVERSAL

Three-terminal geometry



3. JOSEPHSON CURRENT REVERSAL

Three-terminal geometry

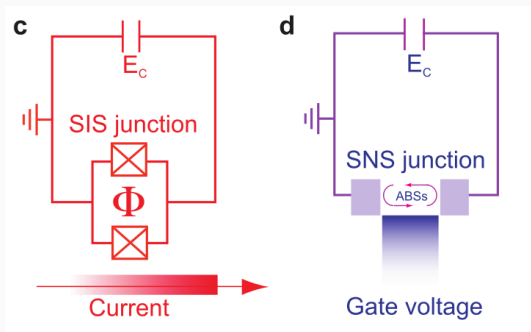


Reversal of dc Josephson current at certain phase difference ϕ is driven by **parity change** of the Andreev bound states of QD.

T. Domański, M. Žonda, V. Pokorný, G. Górski, V. Janiš,
T. Novotný Phys. Rev. B 95, 045104 (2017).

4. SUPERCONDUCTING QUBITS

Schematical view of the superconducting quantum bits in realization of: **transmon** (left) and **gatemon** (right h.s. panel).

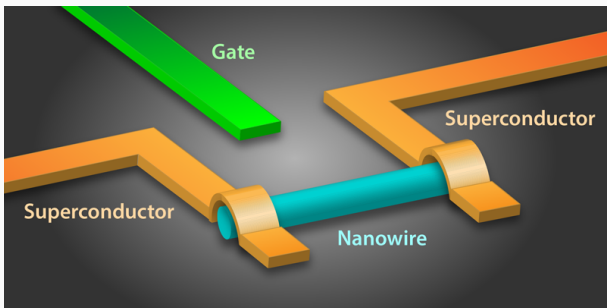


R. Aguado, *Appl. Phys. Lett.* **117**, 240501 (2020).

Superconducting island circuit based on Josephson junction, which is capacitively shunted (E_C is the charging energy).

4. SUPERCONDUCTING QUBITS: GATEMON

Idea: Electrical control over the Josephson supercurrent through semiconducting nanowire accomplished by a side-gate potential.



J.M. Nichol, *Physics* 8, 87 (2015).

5. JOSEPHSON DIODE


The field-free Josephson diode in a van der Waals heterostructure



<https://doi.org/10.1038/s41586-022-04504-8>

Received: 29 March 2021

Accepted: 2 February 2022

Published online: 27 April 2022

 Check for updates

Heng Wu^{1,2,3,6}, Yaojia Wang^{1,3,6}, Yuanfeng Xu^{1,4}, Pranava K. Sivakumar¹, Chris Pasco⁵, Ulderico Filippozzi³, Stuart S. P. Parkin¹, Yu-Jia Zeng², Tyrel McQueen⁵ & Mazhar N. Ali^{1,3}

The superconducting analogue to the semiconducting diode, the Josephson diode, has long been sought with multiple avenues to realization being proposed by theorists^{1–3}. Showing magnetic-field-free, single-directional superconductivity with Josephson coupling, it would serve as the building block for next-generation superconducting circuit technology. Here we realized the Josephson diode by fabricating an inversion symmetry breaking van der Waals heterostructure of NbSe₂/Nb₃Br₈/NbSe₂. We demonstrate that even without a magnetic field, the junction can be superconducting with a positive current while being resistive with a negative current.

Nature | Vol 604 | 28 April 2022 | 653.

5. JOSEPHSON DIODE


The field-free Josephson diode in a van der Waals heterostructure



<https://doi.org/10.1038/s41586-022-04504-8>

Received: 29 March 2021

Accepted: 2 February 2022

Published online: 27 April 2022

 Check for updates

Heng Wu^{1,2,3,6}, Yaojia Wang^{1,3,6}, Yuanfeng Xu^{1,4}, Pranava K. Sivakumar¹, Chris Pasco⁵, Ulderico Filippozzi³, Stuart S. P. Parkin¹, Yu-Jia Zeng², Tyrel McQueen⁵ & Mazhar N. Ali^{1,3,6}

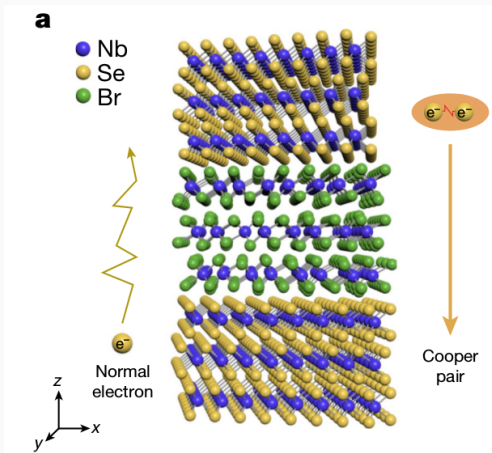
The superconducting analogue to the semiconducting diode, the Josephson diode, has long been sought with multiple avenues to realization being proposed by theorists^{1–3}. Showing magnetic-field-free, single-directional superconductivity with Josephson coupling, it would serve as the building block for next-generation superconducting circuit technology. Here we realized the Josephson diode by fabricating an inversion symmetry breaking van der Waals heterostructure of NbSe₂/Nb₃Br₈/NbSe₂. We demonstrate that even without a magnetic field, the junction can be superconducting with a positive current while being resistive with a negative current.

Nature | Vol 604 | 28 April 2022 | 653.

Discovery of the magnetic field-free superconducting diode in van der Waals heterostructure of NbSe₂/Nb₃Br₈/NbSe₂.

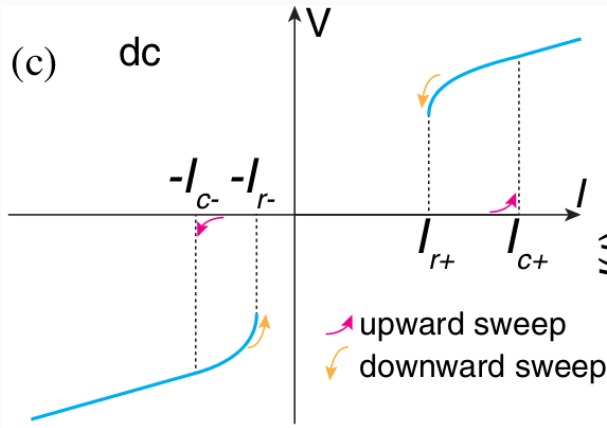
5. JOSEPHSON DIODE

Niobium bromide (just a few atoms thick) placed between layers of superconducting niobium diselenide does conduct electricity without resistance solely in one direction of the applied voltage.



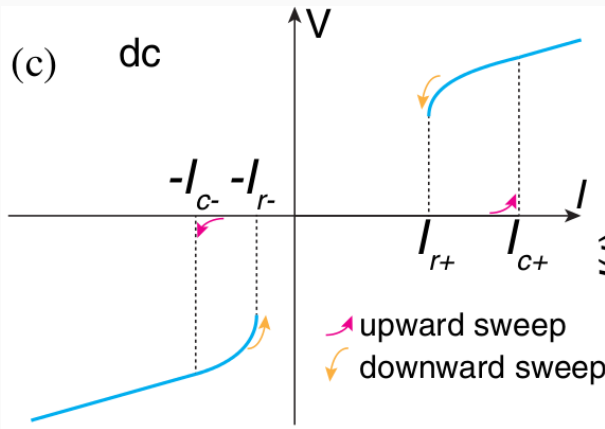
5. JOSEPHSON DIODE

Mechanism behind the Josephson diode effect is not fully understood.



5. JOSEPHSON DIODE

Mechanism behind the Josephson diode effect is not fully understood.

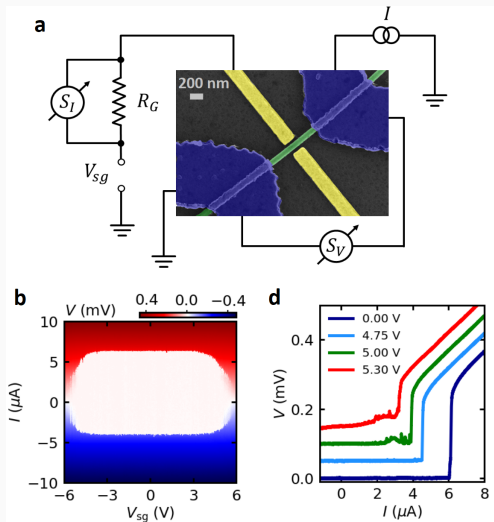


Speculations:

Major role plays the asymmetric sc proximity process inside the tunneling barrier due to: (a) inversion symmetry breaking, (b) time-reversal breaking.

6. JOSEPHSON TRANSISTOR

T. Elalaily, M. Berke, I. Lilja, A. Savin, G. Fülöp, L. Kupás, T. Kanne, J. Nygard, P. Makk, P. Hakonen, S. Csonka, arXiv:2312.15453 (2023).

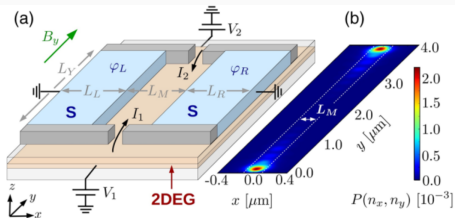


Part 3. Topological superconductivity **(in Josephson junctions)**

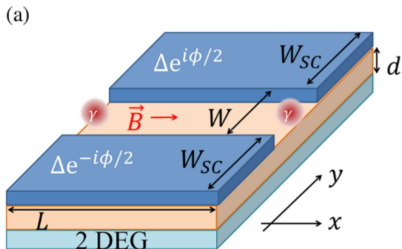
Theoretical concept (2017)

PLANAR JOSEPHSON JUNCTIONS

Idea: Narrow metallic region with the strong spin-orbit interaction and in presence of magnetic field embedded between external superconductors.



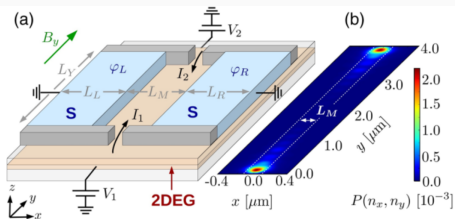
Michael Hell et al., PRL 118, 107701 (2017)



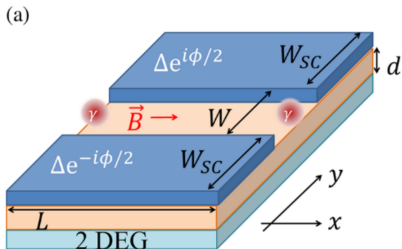
F. Pientka et al., Phys. Rev. X 7,021032 (2017)

PLANAR JOSEPHSON JUNCTIONS

Idea: Narrow metallic region with the strong spin-orbit interaction and in presence of magnetic field embedded between external superconductors.



Michael Hell et al., PRL 118, 107701 (2017)



F. Pientka et al., Phys. Rev. X 7,021032 (2017)

Benefit:

Phase-tunable topological superconductivity induced in the metallic stripe.

PLANAR JOSEPHSON JUNCTIONS

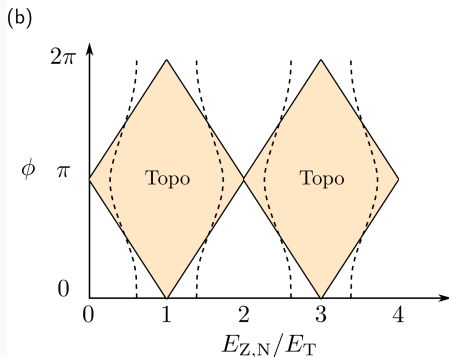
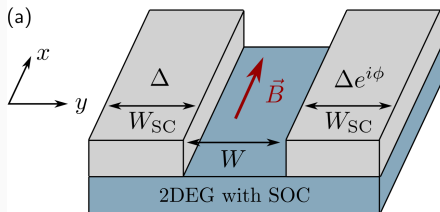
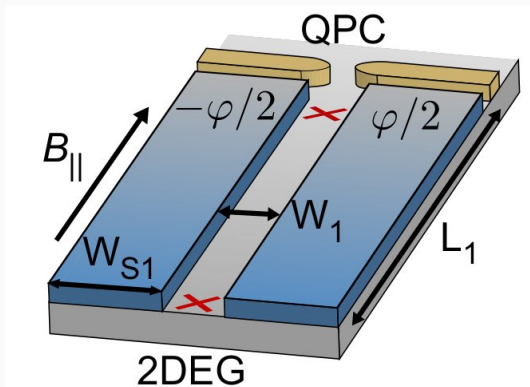


Diagram of topological superconducting state vs
– phase difference ϕ ,
– magnetic field E_z .

Experimental realization (2019)

PLANAR JOSEPHSON JUNCTIONS

Two-dimensional electron gas of **InAs** epitaxially covered by a thin **Al** layer



Width:

$$W_1 = 80 \text{ nm}$$

Length:

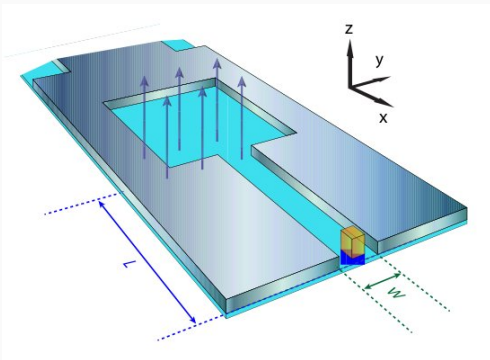
$$L_1 = 1.6 \text{ } \mu\text{m}$$

A. Fornieri, ..., [Ch. Marcus](#) and [F. Nichele](#), *Nature* **569**, 89 (2019).

Niels Bohr Institute (Copenhagen, Denmark)

PLANAR JOSEPHSON JUNCTIONS

Two-dimensional **HgTe** quantum well coupled to 15 nm thick **Al** film



Width:

$$W = 600 \text{ nm}$$

Length:

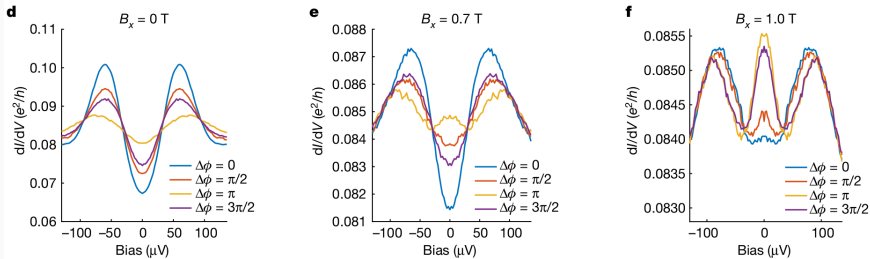
$$L = 1.0 \text{ } \mu\text{m}$$

H. Ren, ..., [L.W. Molenkamp](#), B.I. Halperin & A. Yacoby, *Nature* **569**, 93 (2019).

Würzburg Univ. (Germany) + Harvard Univ. (USA)

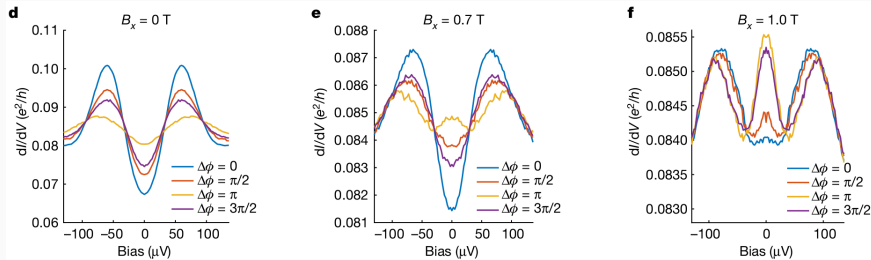
PLANAR JOSEPHSON JUNCTION: EXPERIMENT

H. Ren, ..., [L.W. Molenkamp](#), B.I. Halperin & A. Yacoby, *Nature* **569**, 93 (2019).

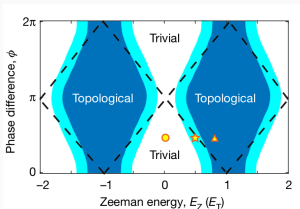


PLANAR JOSEPHSON JUNCTION: EXPERIMENT

H. Ren, ..., [L.W. Molenkamp](#), B.I. Halperin & A. Yacoby, *Nature* **569**, 93 (2019).



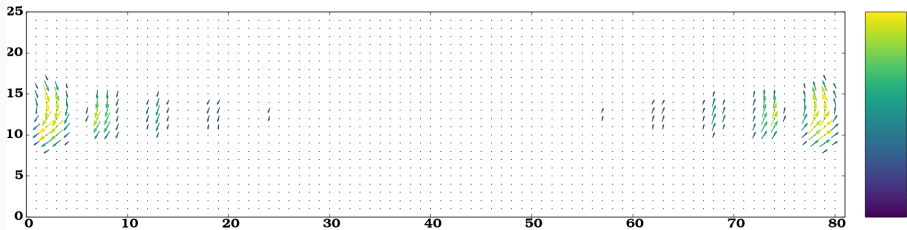
Experimental data obtained for three different magnetic fields indicated by the symbols in phase diagram \Rightarrow .



Topography of Majorana modes

TOPOGRAPHY OF MAJORANA MODES

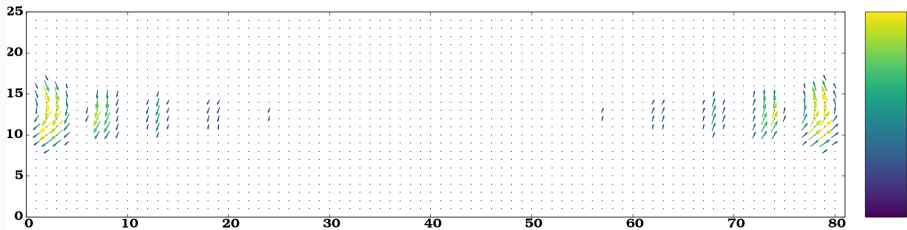
Spatial profile of the zero-energy quasiparticles of a homogeneous metallic strip embedded into the Josephson junction obtained for the phase difference $\phi = \pi$, that is optimal for topological state.



“Majorana polarization vector” $u_{\uparrow,n}v_{\uparrow,n} - u_{\downarrow,n}v_{\downarrow,n}$ obtained for the quasiparticle eigenvalue $E_n = 0$.

TOPOGRAPHY OF MAJORANA MODES

Spatial profile of the zero-energy quasiparticles of a homogeneous metallic strip embedded into the Josephson junction obtained for the phase difference $\phi = \pi$, that is optimal for topological state.

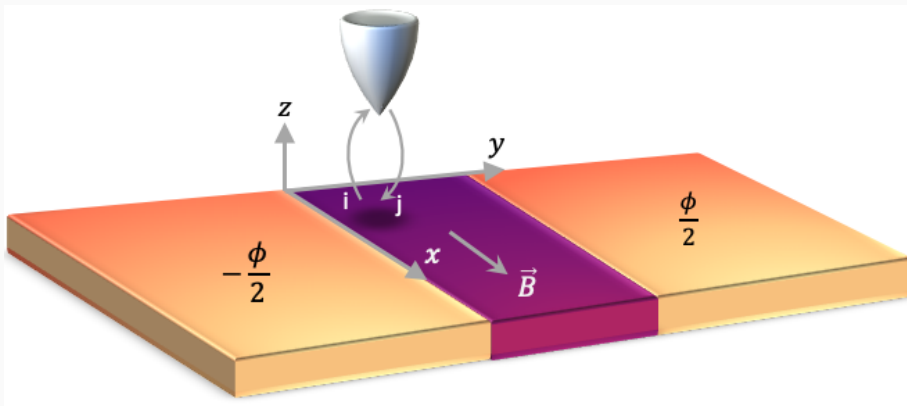


“Majorana polarization vector” $u_{\uparrow,n}v_{\uparrow,n} - u_{\downarrow,n}v_{\downarrow,n}$ obtained for the quasiparticle eigenvalue $E_n = 0$. **Magnitude of this quantity is measurable by the conductance of SESAR spectroscopy.**

Sz. Głodzik, N. Sedlmayr & T. Domański, PRB [102](#), 085411 (2020).

TOPOGRAPHY OF MAJORANA MODES

Selective Equal Spin Andreev Reflection (SESAR) spectroscopy:

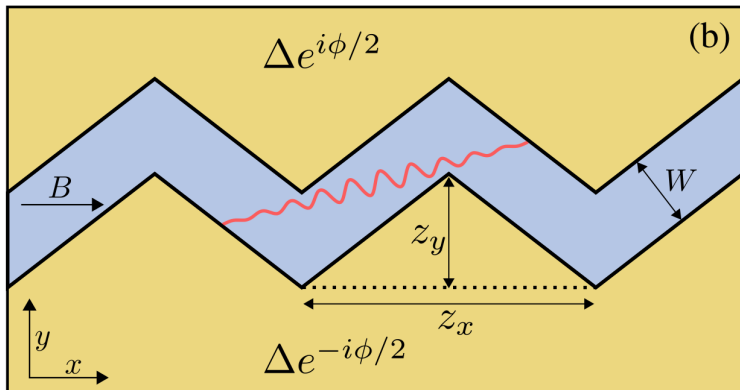


Sz. Głodzik, N. Sedlmayr & T. Domański, PRB 102, 085411 (2020).

Means to localize Majoranas

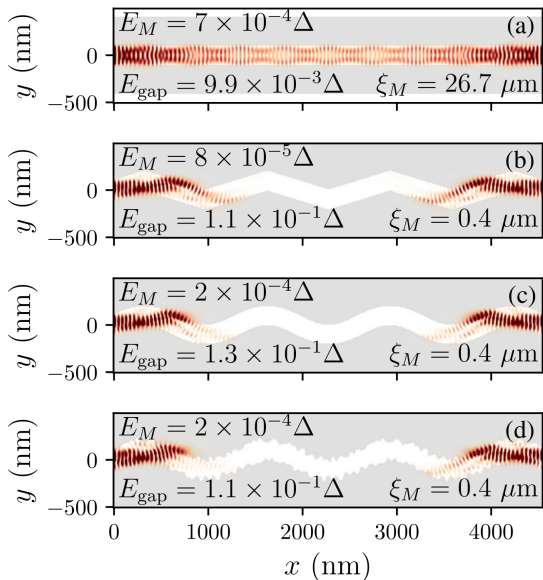
I. DESHAPED JOSEPHSON JUNCTION

To reduce spatial extent of the Majorana modes and increase the topological gap one can use zigzag-shape metallic stripe.



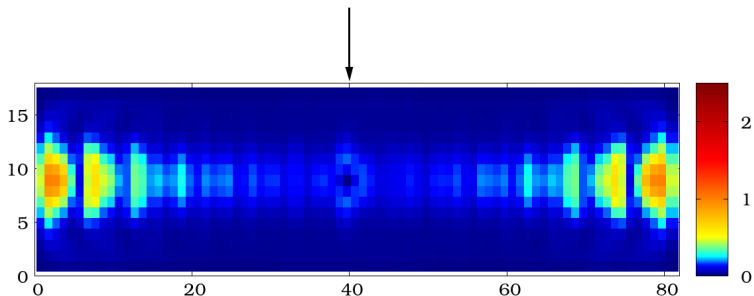
T. Laeven, B. Nijholt, M. Wimmer & A.R. Akhmerov, PRL 102, 086802 (2020).

I. DESHAPED JOSEPHSON JUNCTION



II. LOCAL DEFECT IN JOSEPHSON JUNCTION

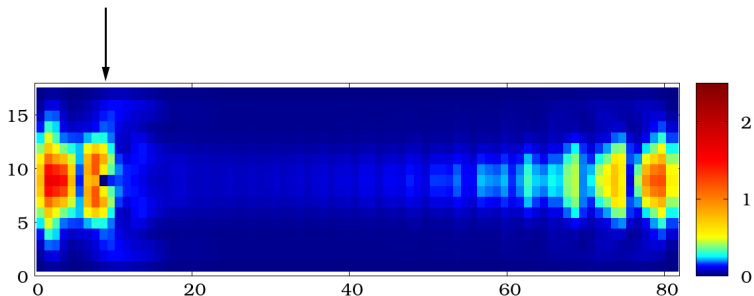
Spatial profile of the Majorana modes in presence of the strong electrostatic defect placed **in the center**.



Sz. Głodzik, N. Sedlmayr & T. Domański, PRB 102, 085411 (2020).

II. LOCAL DEFECT IN JOSEPHSON JUNCTION

Spatial profile of the Majorana modes in presence of the strong electrostatic defect placed **near the edge**.



Sz. Głodzik, N. Sedlmayr & T. Domański, PRB [102](#), 085411 (2020).

III. RANDOM DISORDER

"Benefits of Weak Disorder in dim=1 Topological Superconductors"

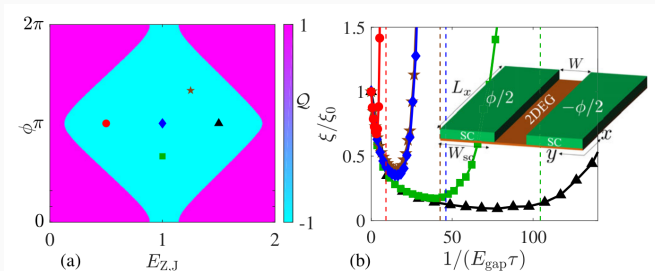
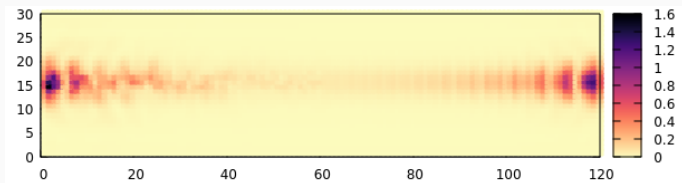


FIG. 1. (a) Phase diagram of the planar Josephson junction Eq. (1) in the clean limit. In the topological phase ($Q = -1$), the system supports zero-energy MBSs at each end of the junction. (b) The Majorana localization length ξ versus the disorder-induced inverse mean free time τ^{-1} for different points inside the topological phase [see markers in (a)].

A. Haim & A. Stern, Phys. Rev. Lett. 122, 126801 (2019).

III. RANDOM DISORDER

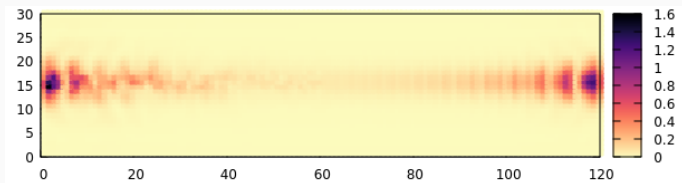
The left-hand-side part of the metallic stripe is randomly disordered



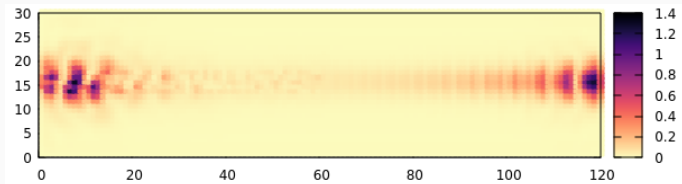
weak disorder

III. RANDOM DISORDER

The left-hand-side part of the metallic stripe is randomly disordered



weak disorder



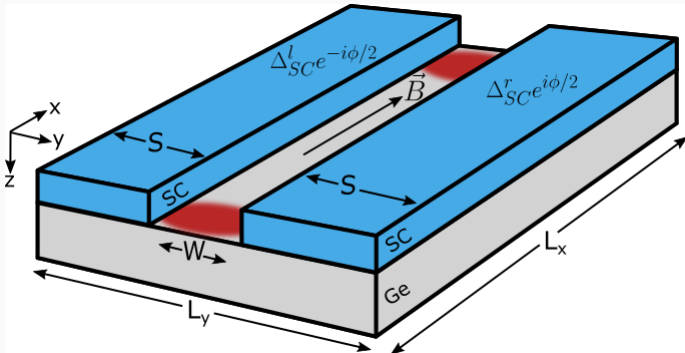
moderate disorder

Sz. Głodzik, N. Sedlmayr & T. Domański, PRB 102, 085411 (2020).

New proposals

1. GERMANIUM BASED PLANAR JJ

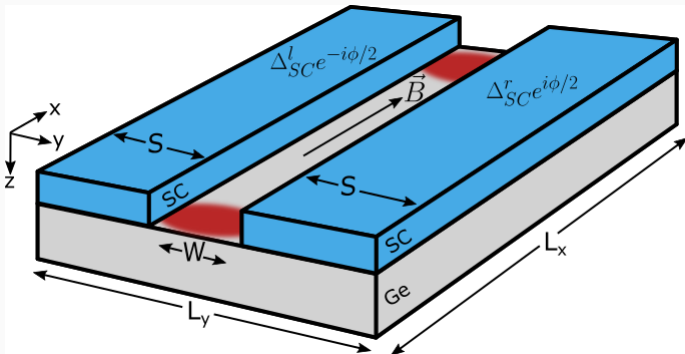
2D hole gas of germanium (Ge) exhibits strong and tunable spin-orbit interaction (cubic in momentum). Such Ge structures can be compatible with the existing metal-oxide-semiconductor (CMOS) technology.



M. Luethi, K. Laubscher, S. Bosco, D. Loss & J. Klinovaja, PRB 107, 035435 (2023).

1. GERMANIUM BASED PLANAR JJ

2D hole gas of germanium (Ge) exhibits strong and tunable spin-orbit interaction (cubic in momentum). Such Ge structures can be compatible with the existing metal-oxide-semiconductor (CMOS) technology.

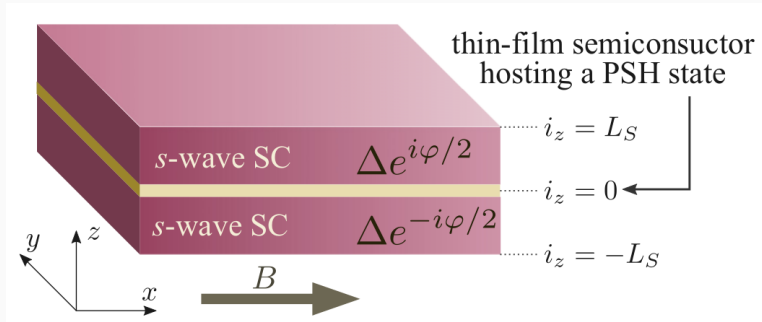


M. Luethi, K. Laubscher, S. Bosco, D. Loss & J. Klinovaja, PRB 107, 035435 (2023).

⇒ **topological phase is asymmetric on phase reversal $\phi \rightarrow -\phi$**

2. VERTICAL JOSEPHSON JUNCTION

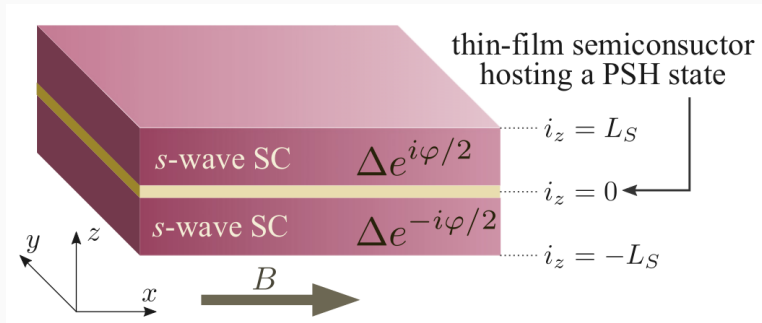
Josephson junction, comprising a thin semiconducting film sandwiched between conventional s-wave superconductors.



D. Oshima, S. Ikegaya, A.P. Schnyder & Y. Tanaka, *Phys. Rev. Research* **4**, L022051 (2022).

2. VERTICAL JOSEPHSON JUNCTION

Josephson junction, comprising a thin semiconducting film sandwiched between conventional s-wave superconductors.

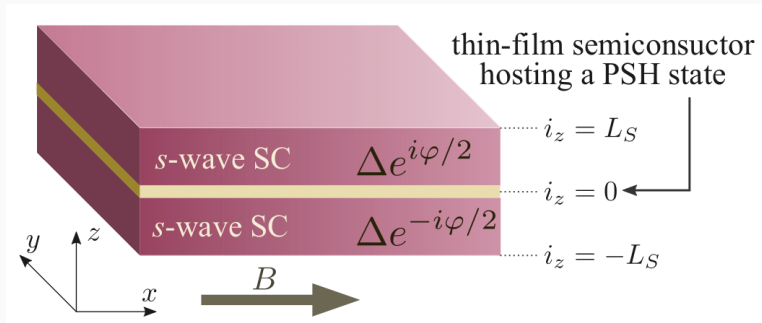


D. Oshima, S. Ikegaya, A.P. Schnyder & Y. Tanaka, Phys. Rev. Research **4**, L022051 (2022).

\Rightarrow **semiconducting region hosts a Persistent Spin-Helix state**

2. VERTICAL JOSEPHSON JUNCTION

Josephson junction, comprising a thin semiconducting film sandwiched between conventional s-wave superconductors.



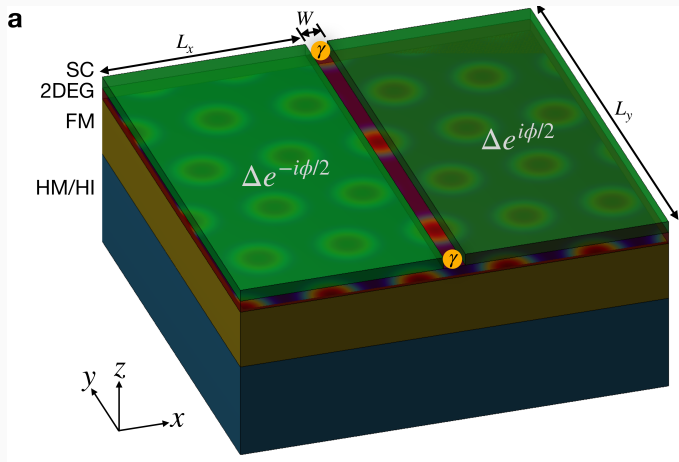
D. Oshima, S. Ikegaya, A.P. Schnyder & Y. Tanaka, Phys. Rev. Research **4**, L022051 (2022).

⇒ **semiconducting region hosts a Persistent Spin-Helix state**

⇒ **a weak Zeeman field can induce p_x -wave superconductivity**

3. SKYRMIONS UNDER JOSEPHSON JUNCTION

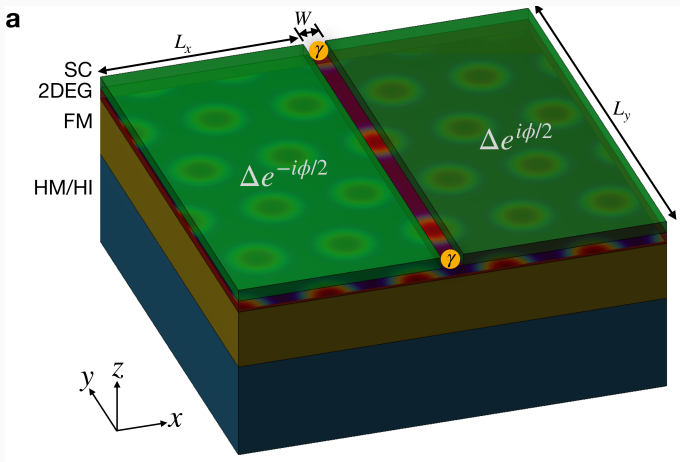
Josephson junction deposited on top of a skyrmion crystal.



N. Mohanta, S. Okamoto & E. Dagotto, *Communications Physics* **4**, 163 (2021).

3. SKYRMIONS UNDER JOSEPHSON JUNCTION

Josephson junction deposited on top of a skyrmion crystal.

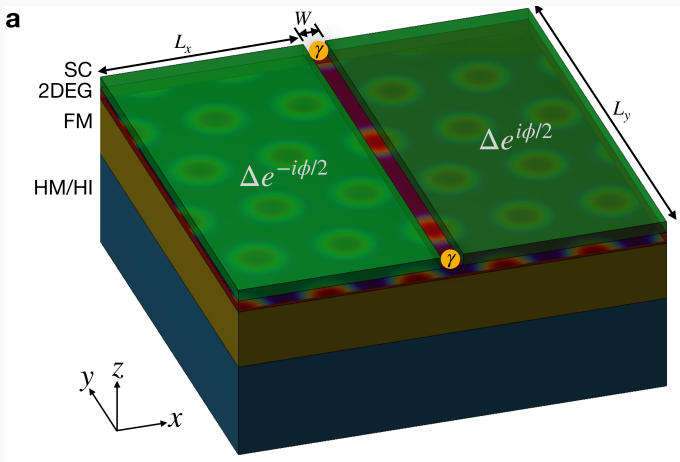


N. Mohanta, S. Okamoto & E. Dagotto, *Communications Physics* **4**, 163 (2021).

FM - ferromagnetic layer

3. SKYRMIONS UNDER JOSEPHSON JUNCTION

Josephson junction deposited on top of a skyrmion crystal.

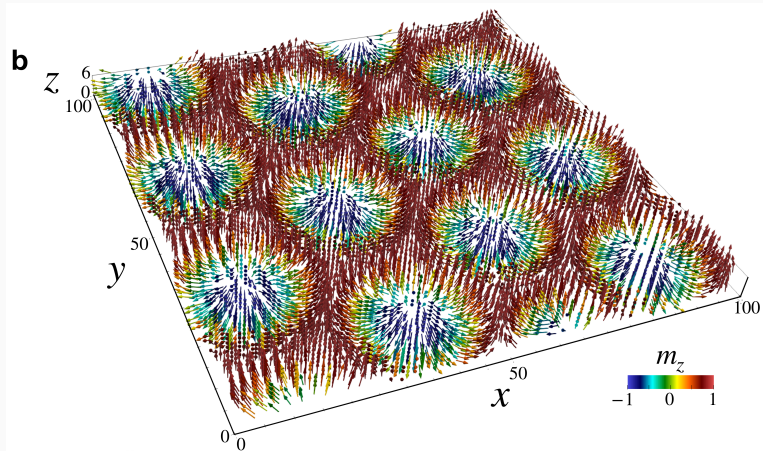


N. Mohanta, S. Okamoto & E. Dagotto, *Communications Physics* **4**, 163 (2021).

FM - ferromagnetic layer **HM/HI - heavy metal or heavy insulator**

3. SKYRMIONS UNDER JOSEPHSON JUNCTION

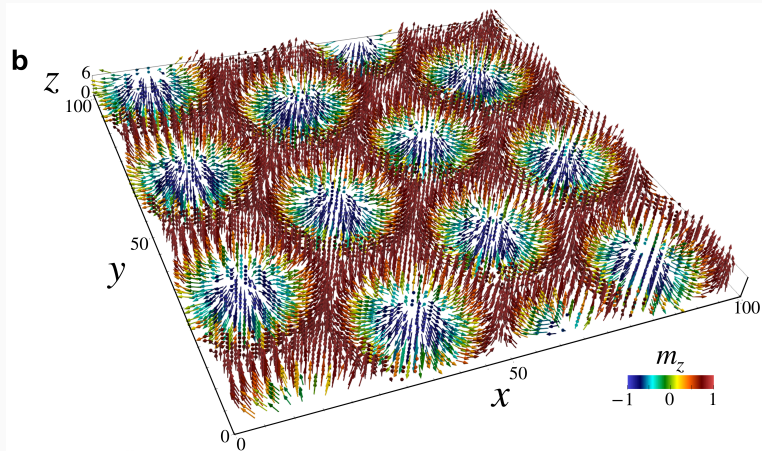
N. Mohanta, S. Okamoto & E. Dagotto, *Communications Physics* **4**, 163 (2021).



Skymions are driven in FM region by:

3. SKYRMIONS UNDER JOSEPHSON JUNCTION

N. Mohanta, S. Okamoto & E. Dagotto, *Communications Physics* **4**, 163 (2021).

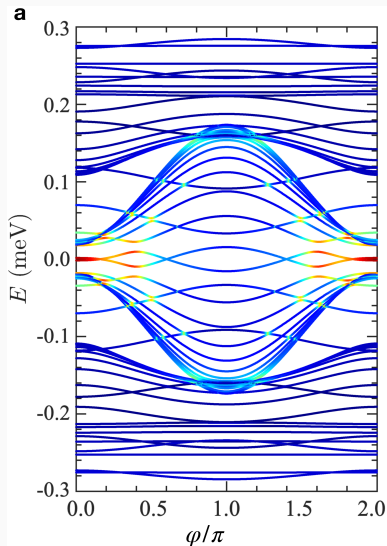


Skyrmions are driven in FM region by: ★ ferromagnetic exchange

★ Dzyaloshinskii-Moriya interaction ★ magnetic field

3. SKYRMIONS UNDER JOSEPHSON JUNCTION

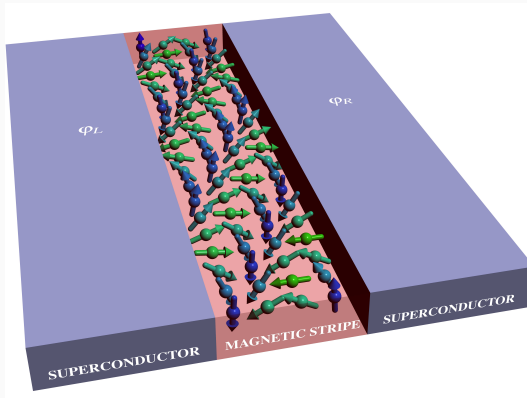
N. Mohanta, S. Okamoto & E. Dagotto, *Communications Physics* **4**, 163 (2021).



Phase difference has detrimental influence on the Majorana modes.

4. JJ WITH SELFORGANIZED MAGNETIC STRIPE

Narrow metallic stripe with the classical magnetic moments placed between two s-wave superconductors, differing in phase $\phi_L \neq \phi_R$.

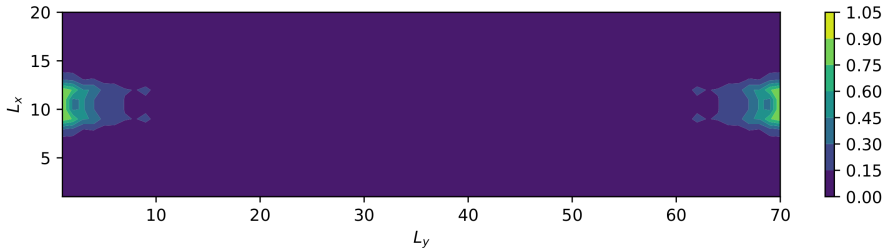


M.M. Maška, M. Dziurawiec & N. Sedlmayr, T.D. – work in progress

/ Technical University (Wrocław) & UMCS (Lublin) cooperation/

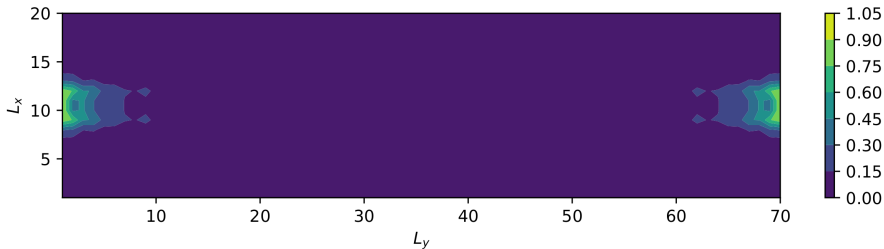
4. JJ WITH SELFORGANIZED MAGNETIC STRIPE

Classical moments of the metallic region develop such magnetic textures, which support the topological superconducting state.



4. JJ WITH SELFORGANIZED MAGNETIC STRIPE

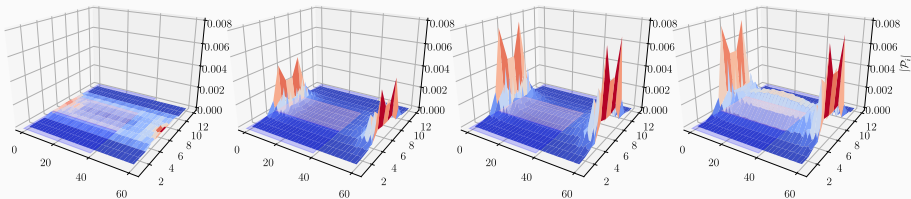
Classical moments of the metallic region develop such magnetic textures, which support the topological superconducting state.



Spatial profile of the Majorana modes – preliminary results obtained for the coplanar magnetic moments.

4. JJ WITH SELFORGANIZED MAGNETIC STRIPE

Topography of the Majorana quasiparticles obtained for the coplanar moments and for various Josephson phase differences $\phi_R - \phi_L$.



$$\phi_R - \phi_L = 0.6\pi$$

$$\phi_R - \phi_L = 0.4\pi$$

$$\phi_R - \phi_L = 0.2\pi$$

$$\phi_R - \phi_L = 0.0$$

Details will be provided tomorrow by: **M.M. Maška**

SUMMARY

Josephson junctions can be used as a platform for realization of the bound states:

SUMMARY

Josephson junctions can be used as a platform for realization of the bound states:

\Rightarrow either conventional (Andreev-type),

SUMMARY

Josephson junctions can be used as a platform for realization of the bound states:

\Rightarrow either conventional (Andreev-type),

\Rightarrow or topological (Majorana-type).

SUMMARY

Josephson junctions can be used as a platform for realization of the bound states:

⇒ either conventional (Andreev-type),

⇒ or topological (Majorana-type).

Both types are promising candidates for stable qubits and/or future quantum computations

SUMMARY

Josephson junctions can be used as a platform for realization of the bound states:

⇒ either conventional (Andreev-type),

⇒ or topological (Majorana-type).

Both types are promising candidates for stable qubits and/or future quantum computations

<http://kft.umcs.lublin.pl/doman/lectures>

ACKNOWLEDGEMENTS

⇒ **Maciek Maśka & coworkers**
(Technical University, Wrocław)



⇒ **Szczepan Głodzik**
(M. Curie-Skłodowska University, Lublin)



⇒ **Nick Sedlmayr**
(M. Curie-Skłodowska University, Lublin)



⇒ **Aksel Kobiałka**
(University of Uppsala, Sweden)



SINGLY OCCUPIED VS BCS-TYPE CONFIGURATIONS

The proximitized quantum dot can be described by

$$\hat{H}_{QD} = \sum_{\sigma} \epsilon_d \hat{d}_{\sigma}^{\dagger} \hat{d}_{\sigma} + U_d \hat{n}_{d\uparrow} \hat{n}_{d\downarrow} - \left(\Delta_d \hat{d}_{\uparrow}^{\dagger} \hat{d}_{\downarrow}^{\dagger} + \text{h.c.} \right)$$

SINGLY OCCUPIED VS BCS-TYPE CONFIGURATIONS

The proximitized quantum dot can be described by

$$\hat{H}_{QD} = \sum_{\sigma} \epsilon_d \hat{d}_{\sigma}^{\dagger} \hat{d}_{\sigma} + U_d \hat{n}_{d\uparrow} \hat{n}_{d\downarrow} - \left(\Delta_d \hat{d}_{\uparrow}^{\dagger} \hat{d}_{\downarrow}^{\dagger} + \text{h.c.} \right)$$

Eigen-states of this problem are represented by:

$$\begin{array}{ll} |\uparrow\rangle \quad \text{and} \quad |\downarrow\rangle & \Leftarrow \quad \text{doublet states (spin } \frac{1}{2}) \\ \left. \begin{array}{l} u |0\rangle - v |\uparrow\downarrow\rangle \\ v |0\rangle + u |\uparrow\downarrow\rangle \end{array} \right\} & \Leftarrow \quad \text{singlet states (spin 0)} \end{array}$$

SINGLY OCCUPIED VS BCS-TYPE CONFIGURATIONS

The proximitized quantum dot can be described by

$$\hat{H}_{QD} = \sum_{\sigma} \epsilon_d \hat{d}_{\sigma}^{\dagger} \hat{d}_{\sigma} + U_d \hat{n}_{d\uparrow} \hat{n}_{d\downarrow} - \left(\Delta_d \hat{d}_{\uparrow}^{\dagger} \hat{d}_{\downarrow}^{\dagger} + \text{h.c.} \right)$$

Eigen-states of this problem are represented by:

$$\begin{array}{ll} |\uparrow\rangle \quad \text{and} \quad |\downarrow\rangle & \Leftarrow \quad \text{doublet states (spin } \frac{1}{2} \text{)} \\ \left. \begin{array}{l} u |0\rangle - v |\uparrow\downarrow\rangle \\ v |0\rangle + u |\uparrow\downarrow\rangle \end{array} \right\} & \Leftarrow \quad \text{singlet states (spin 0)} \end{array}$$

Upon varying the parameters ϵ_d , U_d or Γ_S there can be induced **quantum phase transition** between these doublet/singlet states.